COBEM 2023
27TH INTERNATIONAL CONGRESS OF MECHANICAL ENGINEERING

ABCM
Brazilian Society of Mechanical Sciences and Engineering
27th ABCM International Congress of Mechanical Engineering
December 04-08, 2023, Florianópolis-SC, Brazil

COB-2023-1943
PERMANENT REGIME CONFIGURATIONS FOR ORTHOGONAL CUTTING ANALYSIS BY LIMIT ANALYSIS

Luísa de Amorim Makhoul Gomes
Lavínia Maria Alves Borges
Fabio da Costa Figueiredo
Federal University of Rio de Janeiro, Rio de Janeiro, Brazil
luisa.makhoul@mecanica.coppe.ufrj.br
lavinia@mecanica.coppe.ufrj.br
fabiofigueiredo@mecanica.coppe.ufrj.br

Adriane Lopes Mougo
Federal Center for Technological Education Celso Suckow da Fonseca, Campus Nova Iguaçu, Rio de Janeiro, Brazil
adriane.mougo@cefet-rj.br

Abstract. *This work deals with application of limit analysis theory considering frictional interfaces in the study of orthogonal cutting. Dissimilar to incremental methods, this approach is a direct method, posed as an optimization problem. In limit analysis, a permanent regime configuration is required. Regarding orthogonal cutting, this configuration is not known a priory and its determination depends on the understanding of mechanics of chip formation. However, the determination of this configuration is difficult, since it must fit the velocity field and the primary shear zone, to be analyzed using the limit analysis formulation. This cutting process is influenced by several factors, such as friction, plastic strain, and tool-chip contact length and interface, impacting the cutting dynamics, the tool life and its integrity and the surface finishing. There are many factors not fully understood, then, studying them considering the orthogonal cutting is convenient. When compared to oblique cutting, orthogonal cutting is a relative simple process. However, this process is still under study because it requires fewer parameters and allows for numerical modeling as a planar problem. Experimental procedures to study this process are limited for obtaining the shear angle in the primary shear zone and the contact between the chip and the tool in the secondary shear zone, requiring sophisticated equipment and analytical models, which are costly and time-consuming. Therefore, numerical models are more suitable for this purpose. The proposed numerical simulation is carried out by discretizing the specimen into finite elements and application of limit analysis theory. Permanent regimes configurations can be determined from proposed models found in literature, such as Merchant and Molinari. The objective is to study an orthogonal cutting model that best meets a permanent regime configuration, so that the proposed shape for the chip flow fits with the velocity field obtained by the solution of limit analysis problem. Furthermore, this paper was divided into three parts: First, the cutting forces obtained by the Merchant and Molinari models will be compared with the experimental results for two rake angle, 0 and -6º, and two contact length model found in the literature. After, the shape angle in free chip surface by Molinari model will be analyzed and compared to determined the best using the velocity fields from Molinari Model. Finally, the optimal shear angle for the Merchant model will be proposed and measured from the plastic dissipation results and, later, the cutting forces results will be compared with the theoretically shear angle obtained.*

Keywords: *orthogonal cutting, numerical model, limit analysis, shear angle*

1. INTRODUCTION

Orthogonal cutting process is defined as the cutting type that the tool advances on the workpiece perpendicularly, without any inclination. It is one of the simplifications most used to study machining processes and usually the first hypothesis used to analyses and explain gaps, because these are influenced by complex phenomena like: elasticity, metallurgy, plasticity, heat transfer and tribology (Dimas, 2018).

The first model for orthogonal cutting was proposed by Merchant (1945a,b) and was designed for continuous chip without built-up edge (BUE) and for sharp tool, without tool nose radius. In these studies, the primary shear zone is described, but in this hypothesis it can be simplified as a plane. Using the minimum cutting energy principle to find the shear angle, where the stress in this plane is maximum and assuming the hypothesis that the shear stress τ is a function of the material only machined. Other aspects are introduced in this model, the machining forces can be defined from the decomposition of pair of forces in the Merchant circle for each shear zones and a model for calculating the shear angle as a function of the rake tool and friction angles (Araujo *et al.*, 2020).

After Merchant (1945a,b), others authors have proposed others models, including the Lee and Shaffer model, which presents an update of the shear plane for continuous chips with or without the formation of built-up edge (BUE) using the slip-line method for linear problems (Melkote *et al.*, 2022) and the Molinari and Moufki (2008) model that reviews the chip formation model by Merchant based in the criterion of minimization of the cutting energy, proposing a new chip geometry and with this new configuration changed the shear angle equation. They introduce a perturbation zone on the chip free surface that is influenced by the shape angle and perturbation amplitude, called a stability criterion of the chip morphology.

Studies in machining have extensively focused on experimental, empirical, and analytical methodologies, leading to advances in the field. Numerous experiments were carried out, from evaluation of the evolution of machining parameters and conditions, of different types of metal alloys, the wear and life of the cutting tool. Formulation of empirical and analytical equations aims to estimate phenomena through mathematical deductions and analysis of the physical environment and boundary conditions (Özel and Zeren, 2005), such as to predict machining forces, residual stresses, friction coefficient and chip-tool contact length. The disadvantages of relying solely on experimental methods for analyzing the process include high costs and time consumption due to the necessity of machining numerous specimens and relying on specialized equipment (Özel and Zeren, 2005). Additionally, analytical and empirical methods may be constrained by highly specific conditions for certain formulations.

The use of numerical models to simulate cutting operations may help the understanding of the phenomena and the observation of local responses, not captured by experimental devices. Once calibration such models, other cutting conditions may be evaluated by computational simulation. One of these techniques, limit analysis takes place. According to Figueiredo and Borges (2020), limit analysis theory is a direct method and is convenient if the interest is determination of the ultimate load-carrying of a body or structure: the plastic collapse at a permanent regime configuration. This state is achieved by looking directly at plastic collapse state without any need to follow loading steps as in incremental methods. In this work, a limit analysis methodology considering frictional contact between a rigid (tool) and a deformable body (workpiece) is considered. The permanent regime configuration are determined by Merchant and Molinari models. As results, the cutting forces, plastic dissipation and velocity fields are evaluated. The workpiece is a von Mises material under plane strain hypothesis and Coulomb friction law is used at chip-tool interface.

Based on these premises, the aim of this paper is to study an orthogonal cutting model, Merchant and Molinari, that best meets a permanent regime configuration, so that the proposed shape for the chip flow fits with the velocity field obtained by the solution of limit analysis problem. This paper was divided into three parts: First, the cutting forces obtained by the models will be compared with the experimental results for two rake angle, 0 and -6^o, and two contact length model found in the literature. After, the shape angle will be analyzed and compared to determined the best using the velocity fields from Molinari Model. Finally, the optimal shear angle for the Merchant model will be proposed and measured from the plastic dissipation results and, later, the cutting forces results will be compared with the theoretically shear angle obtained.

2. ORTHOGONAL CUTTING MODELS

This section explains two orthogonal cutting models presented and discussed in literature: Merchant and Molinari. These configurations are presents as follows:

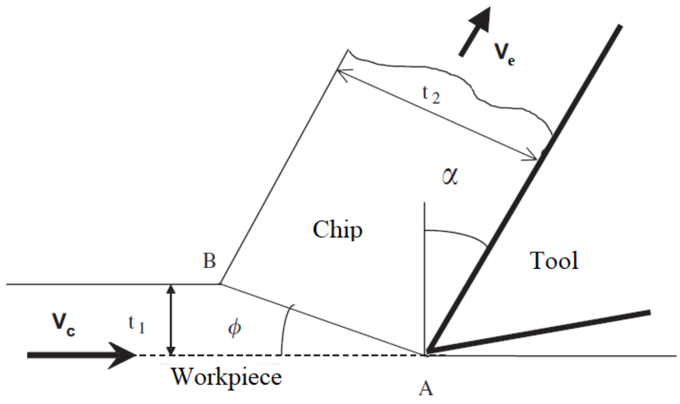

(a) Merchant

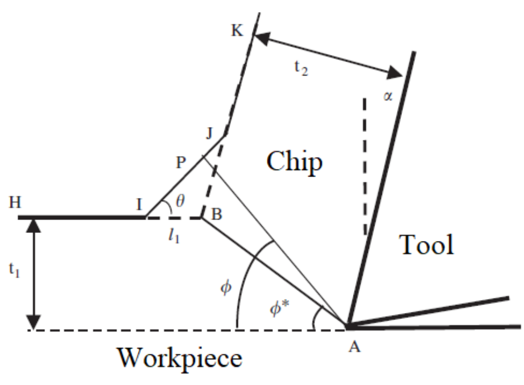

(b) Molinari

Figure 1. Orthogonal cutting models (Molinari and Moufki, 2008).

2.1 Merchant model

The Merchant (1945a,b) model (Fig. 1(a)) was one of the first developed models for orthogonal cutting, this model was idealized for continuous chip without built-up edge and for tools with plane faces, without tool nose radius, ideally sharp and with a single straight cutting edge. This approach considers that the principal strain region is contained in a single plane called the shear plane. This is a simplification of the real process, in which the plastic strain occur on the primary shear region not in a plane (Araujo *et al.*, 2020).

The shear angle model was defined by Ernest e Merchant in 1941, the theory consists of searching the value of the shear angle which the stress in the shear plane is maximum, considering the orthogonal cutting system and continuous chip formation and also admitting the hypothesis that the shear stress τ is a function only of the workpiece material (Ferraresi, 1970). This theory was based on the minimum energy principle, which means that the process demands the lowest power (Araujo *et al.*, 2020; Ebecken, 2009), using this principle the authors proposed the shear angle formulation as function of the friction (β) and rake (α) angles:

$$\phi = \frac{\pi}{4} - \frac{\beta}{2} + \frac{\alpha}{2} \tag{1}$$

2.2 Molinari model

The Molinari and Moufki (2008) model (Fig. 1(b)) proposed a revision of the Merchant model due to the criterion of minimization of the cutting energy used to predict the shear angle, does not generally agree with experimental data and numerical simulations (Molinari and Moufki, 2008). As a way to solve this problem, the authors proposed the addition of a new criterion besides the minimum principal, the stability criterion of the chip morphology.

This model considers the perfectly plastic material orthogonal cutting and that the shear energy is minimized for the virtual velocity fields, defined for the rigid body motion of two blocks. The stability criterion addition a new geometry call perturbation zone, the triangle IBJ in Fig. 1(b) that is influenced by the shape angle (θ), on the free flow surface as a alternative to introduce small perturbations. In this region, there is an optimal value where these two criteria are respected. Thus changing the shear angle and primary shear zone, the new shear angle formulation is shown below as function of the friction, rake and shape angles:

$$\phi_{MM} = \frac{\pi}{4} + \frac{\alpha - \theta - \beta}{2} \tag{2}$$

3. NUMERICAL MODEL

The numerical procedure is based on limit analysis theory considering friction at contact interface as stated in Figueiredo and Borges (2017, 2020). Limit analysis is a direct method based on plasticity theory. Limit analysis aims the determination of the plastic collapse power (in this case it is related to cutting forces), velocity and stresses fields, plastic strain rates and plastic dissipation. In the propose formulation, the occurrence of sticking/sliding regimes at tool-chip interface is determined from the distribution of contact stresses and tangential velocities. If sliding occurs, there is friction dissipation. Otherwise, there is sticking. If sticking occurs, material adheres to rake face and the secondary shear zone is formed.

In the computational model, the workpiece is treated as a deformable body, under the assumptions of elastic perfectly-plastic material, von Mises criteria and in a plane strain hypothesis. The tool is treated as a rigid body, not represent in the model. The contact interface is represented by unilateral conditions, assuming known and permanent contact and Coulomb friction law for tangential direction. The deformable body is discretized into triangular finite elements, considering quadratic interpolation for the velocity field and linear interpolation for the stress field.

In limit analysis, a permanent configuration is required. This configuration is determined from the Mechant's model (Araujo *et al.*, 2020; Groover, 2012), considering the chip as continuous and straight. In orthogonal cutting, large deformation usually occurs. However, dissimilar to incremental analysis in which a load history is imposed and the geometry is updated at each load step, limit analysis deals with the phenomenon of imminent plastic collapse at a permanent regime configuration. In this case, this configuration is determined by Merchant model. In this context, limit analysis deals with strain rates (not strain) in an elastic perfectly-plastic material and the velocity field expresses a tendency of movement at plastic collapse. Limit analysis looks for this limit situation, after that large deformation may occur. The post plastic collapse response is not covered by this theory.

The specimen domain is discretized into triangular finite elements, with quadratic interpolation for the velocity field and linear interpolation for the stress field. An adaptive mesh is presented as follows:

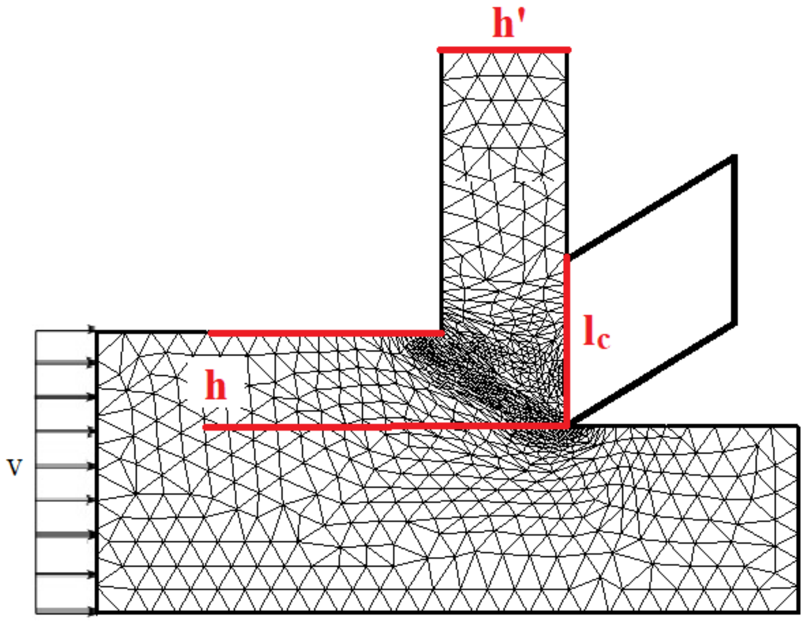

Figure 2. Adaptive mesh for the numerical solution.

A velocity field is imposed in order to simulate the movement of the workpiece, while the cutting tool is stationary.

The contact lengths (l_c) are evaluated from Kachanov and Poletika's model (Grzesik, 2016), presented in the Eq. (3). Equation (3a) is dependent on the shear plane angle (ϕ) (Eq. (1)), whereas Eq. (3b) is dependent on the chip thickness (h') (Grzesik, 2016; Kato *et al.*, 1972).

$$l_c = \frac{2hcos\left(\alpha - \phi\right)}{sen\phi} \quad (3a)$$

$$l_c = 2h' \quad (3b)$$

where h is the nominal thickness of the cut.

To obtain the chip thickness (h'), it is necessary to collect the chip produced during experimental machining and use the Scanning Electron Microscope (SEM) to obtain an image of this chip. Then, the chip thickness is measured with the chip SEM image and using the ImageJ.

In order to generate the Merchant-based geometry, some parameters are necessary: cutting thickness (h = 0.199 mm); friction coefficient (μ); chip-tool contact length (l_c); rake angle surface (α); rotation velocity (n = 800 rpm), chip thickness (h'), cut depth (a_p); cutting width determined by Waldorf (2006) model (w), as shown in Eq. (4), yield stress material (σ_y) and experimental cutting force for these machining conditions (F_c^{exp}).

$$w = r_n\left(\frac{\pi}{2} - \chi' + sen^{-1}\left(\frac{f}{2r_n}\right)\right) + \frac{a_p - r_n\left[1 - sen(\chi')\right]}{cos(\chi')} \quad (4)$$

where χ' is the side cutting edge (lead) angle and r_n is the tool nose radius.

The second geometry was based on the Molinari Model. This model considers the same inputs as in Merchant geometry with the addition of two other parameters, shape angle (θ) and perturbation amplitude (δ_1), which was used 0.05 in order to guarantee the minimum perturbation region as established in Molinari and Moufki (2008).

4. RESULTS AND DISCUSSIONS

This section presents some discussions and results about the Merchant and Molinari orthogonal cutting models. First, the cutting forces were obtained by the numerical model for each configuration and compared with the experimental results. After, velocity fields were analyzed for the two models and specifically for the Molinari were studied the effects of the shape angle variation in the perturbation region. Finally, optimal shear angle were propose for the Merchant configuration using image correlation for measured the new shear angle.

During this work, two experiments data and results from the literature (Gomes *et al.*, 2022; Almeida, 2020) were used for AISI 316 stainless steel, as shown in the Tab. 1:

Table 1. Experimental data (Gomes *et al.*, 2022; Almeida, 2020).

f (mm)	α	F_c^{exp} (N)	μ	l_c (mm)	
0.199	0	92.55	0.2837	Merchant	0.5266
				geometric	0.4076
	-6	68.18	0.0971	Merchant	0.5434
				geometric	0.3640

4.1 Comparison of the cutting forces obtained by the models

Table 2 presents the cutting forces results by the numerical model for Merchant configuration.

Table 2. Cutting forces results by numerical model for Merchant configuration.

α	F_c^{exp} (N)	l_c	$F_c(N)$	Error $(\%)$
0	92.55	Merchant	95.676	-3.38
		geometric	95.187	-2.85
-6	68.18	Merchant	71.164	-4.37
		geometric	72.345	-6.10

These results show that the numerical cutting forces were superior for each case simulated when compared with experimental results, with a maximum error of -3.38% and -6.10%, respectively for the rake angle 0^o and -6^o. Changing contact length models did not have much influence.

The same process were made for the Molinari model, by adding two new parameters: the shape angle (θ) and the perturbation amplitude (δ_1) as a fraction of uncut chip (h), as presents in the Tab. 3.

Table 3. Cutting forces results by numerical model for Molinari configuration.

α	F_c^{exp} (N)	θ	F_c (N)		Error $(\%)$	
			l_c Merc	l_c geo	l_c Merc	l_c geo
0	92.55	15	96.978	96.696	-4.78%	4.48%
		30	96.337	96.259	-4.09%	-4.01%
		45	98.473	96.276	-6.40%	-4.03%
		60	96.033	96.440	-3.76%	-4.20%
		75	96.047	96.396	-3.78%	-4.16%
-6	68.18	15	72.799	70.541	-6.77%	-3.46%
		30	69.723	70.927	-2.26%	-4.02%
		45	71.121	69.221	-4.31%	-1.52%
		60	70.051	74.195	-2.74%	-8.80%
		75	69.732	69.252	-2.27%	-1.57%

From results presented in Tab. 3, one observes little influence of perturbation angle (θ) on cutting forces estimation. The maximum relative errors were 6.40% and 8.8% for rake angles $\alpha = 0^o$ and -6^o respectively. However, the influence of this perturbation angle may be decisive to obtain a permanent regime configuration and fit the velocity field to the geometry of the numerical model.

4.2 Analysis of velocity fields

The influence of the perturbation angle theta can be observed in Fig. 3 and 4. The focus is around the perturbation zone and the verification of the best-fit configuration to the obtained velocity field. The called Merchant configuration corresponds to $\theta = 0$:

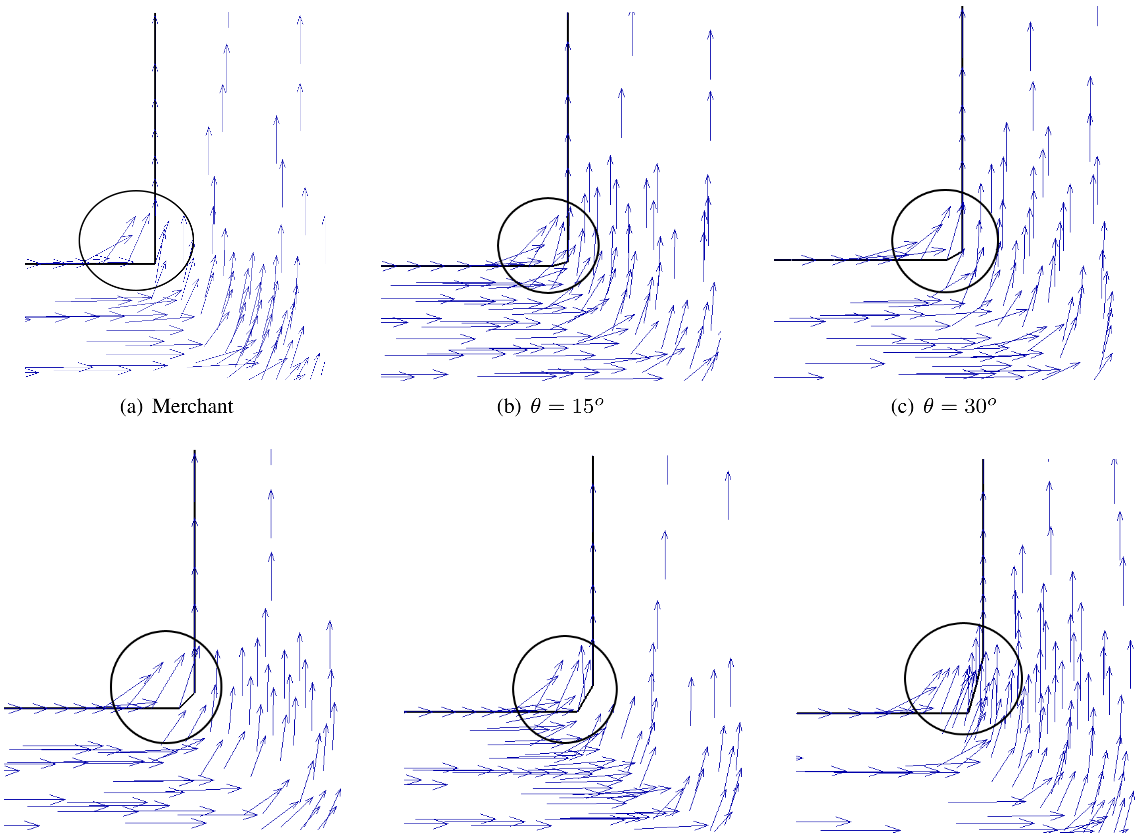

(a) Merchant (b) $\theta = 15^o$ (c) $\theta = 30^o$

(d) $\theta = 45^o$ (e) $\theta = 60^o$ (f) $\theta = 75^o$

Figure 3. Comparison of Merchant and Molinari model velocity fields for $\alpha = 0^o$ and l_c by Merchant.

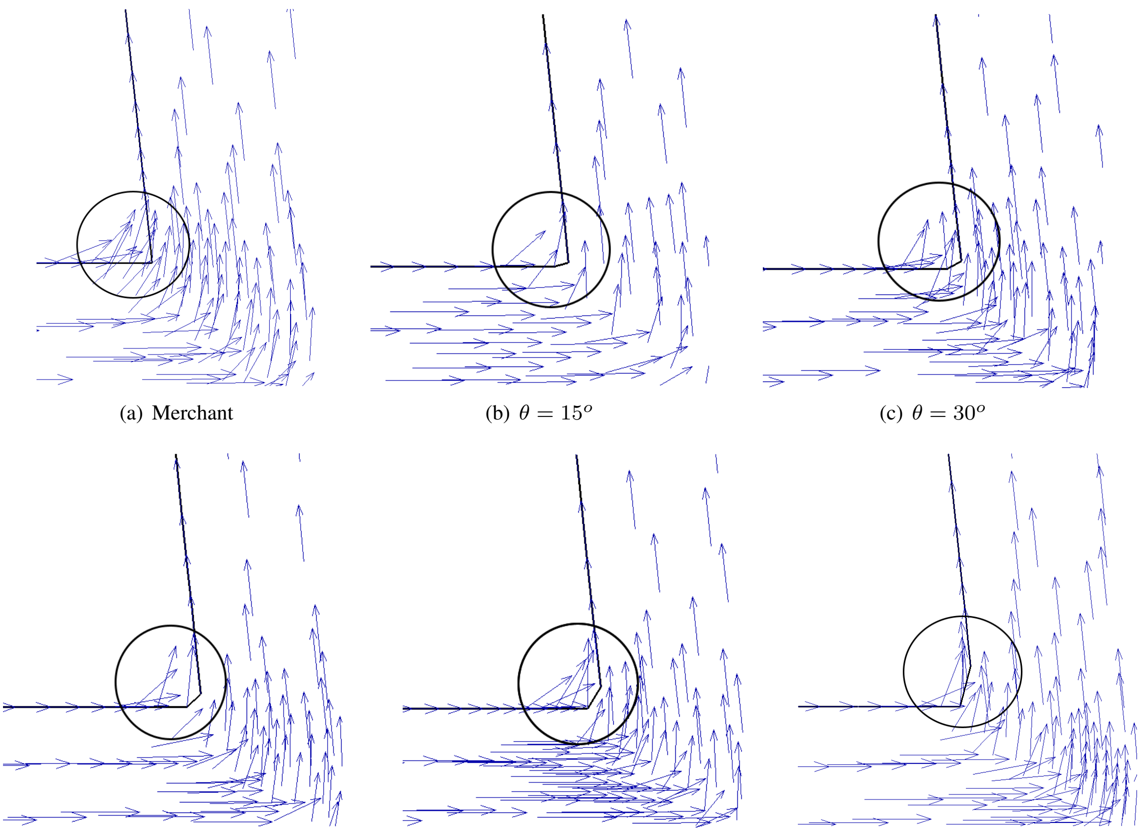

(a) Merchant (b) $\theta = 15^o$ (c) $\theta = 30^o$

(d) $\theta = 45^o$ (e) $\theta = 60^o$ (f) $\theta = 75^o$

Figure 4. Comparison of Merchant and Molinari model velocity fields for $\alpha = -6^o$ and l_c by Merchant.

Analyzing only the free surface, the Merchant Model velocity field is not tangent to the geometry of the permanent regime configuration independent of the rake angle and Molinari model had some cases where the same happens, but dependent of the shape angle and rake angle. For the rake angle 0^o, the best-fit configuration is reached for shape angle 45^o. For rake angle -6^o, 15^o and 45^o.

4.3 Determination of optimal shear angle

In the Molinari and Moufki (2008) works, the Merchant model is discussed with respect to chip morphology. The predicted shear angle (ϕ) in Eq. 1 does not match the experimental observations, and the obtained numerical results present also this evidence, and propose that there is a optimal shear angle that the minimum energy principle and the stability criterion of the chip morphology are respected inside the perturbation region (Fig. 1(b)). With respect to these assumptions, the authors of this work propose determining a new shear angle using the Merchant configuration with plastic dissipation results. These results were then used in conjunction with image correlation through the ImageJ software to obtain the optimal shear angle. Subsequently, the velocity fields and cutting forces were evaluated.

For this propose, the cases presented in Tab. 1 were numerically simulated by limit analysis and finite element methods. Using the plastic dissipation results, the primary shear zone was measured using the ImageJ and then this angle was used for simulate again these cases.

Figure 5 presents these results for the geometric contact length cases:

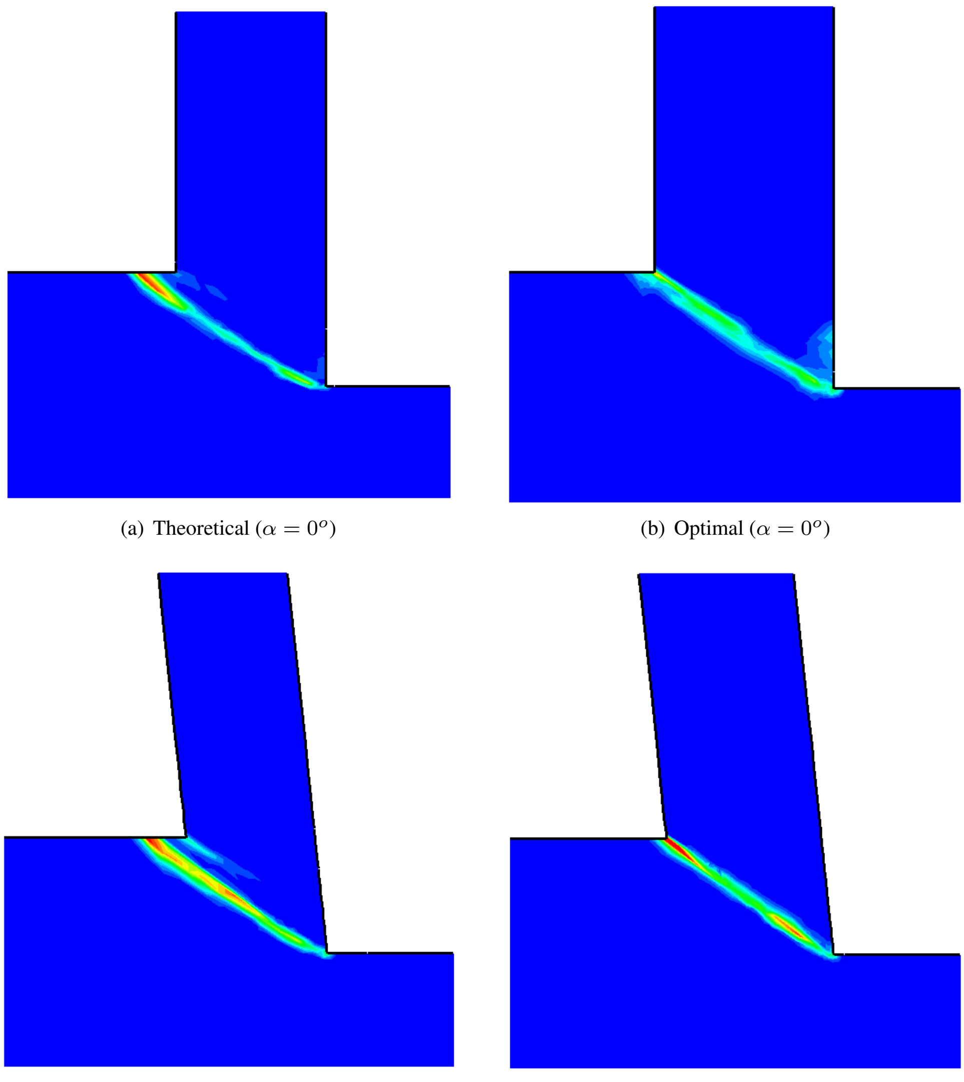

(a) Theoretical ($\alpha = 0^o$) (b) Optimal ($\alpha = 0^o$)

(c) Theoretical ($\alpha = -6^o$) (d) Optimal ($\alpha = -6^o$)

Figure 5. Comparison of theoretical and optimal shear angle configuration plastic dissipation for geometric l_c.

The theoretical shear angle calculated using the Merchant formulation was below the primary shear plane proposed in the Merchant model, as represented by line AB in Fig. 1(a), and this results agrees with the work of Molinari and Moufki (2008). In the same figure, the plastic dissipation results for the optimal angel agree with the Merchant (1945a,b) propose, because the primary shear zone coincides with line AB (except for the case $\alpha = 0^o$ and l_c by Merchant that was a little below the plane).

In the Table 4 there is a comparison between the theoretical and optimal angle:

Table 4. Comparison with theoretical and optimal shear angle results.

α	$\phi_{theoretical}$	l_c	$\phi_{optimal}$	PD (%)
0	37.081	Merchant	34.258	7.61
		geometric	32.869	11.36
-6	39.369	Merchant	34.804	11.60
		geometric	34.645	12.00

The maximum relative difference was 12% or approximately 5^o.

Figure 6 shows the comparison between the theoretical and optimal velocity fields. The velocity fields around perturbation zones are detached:

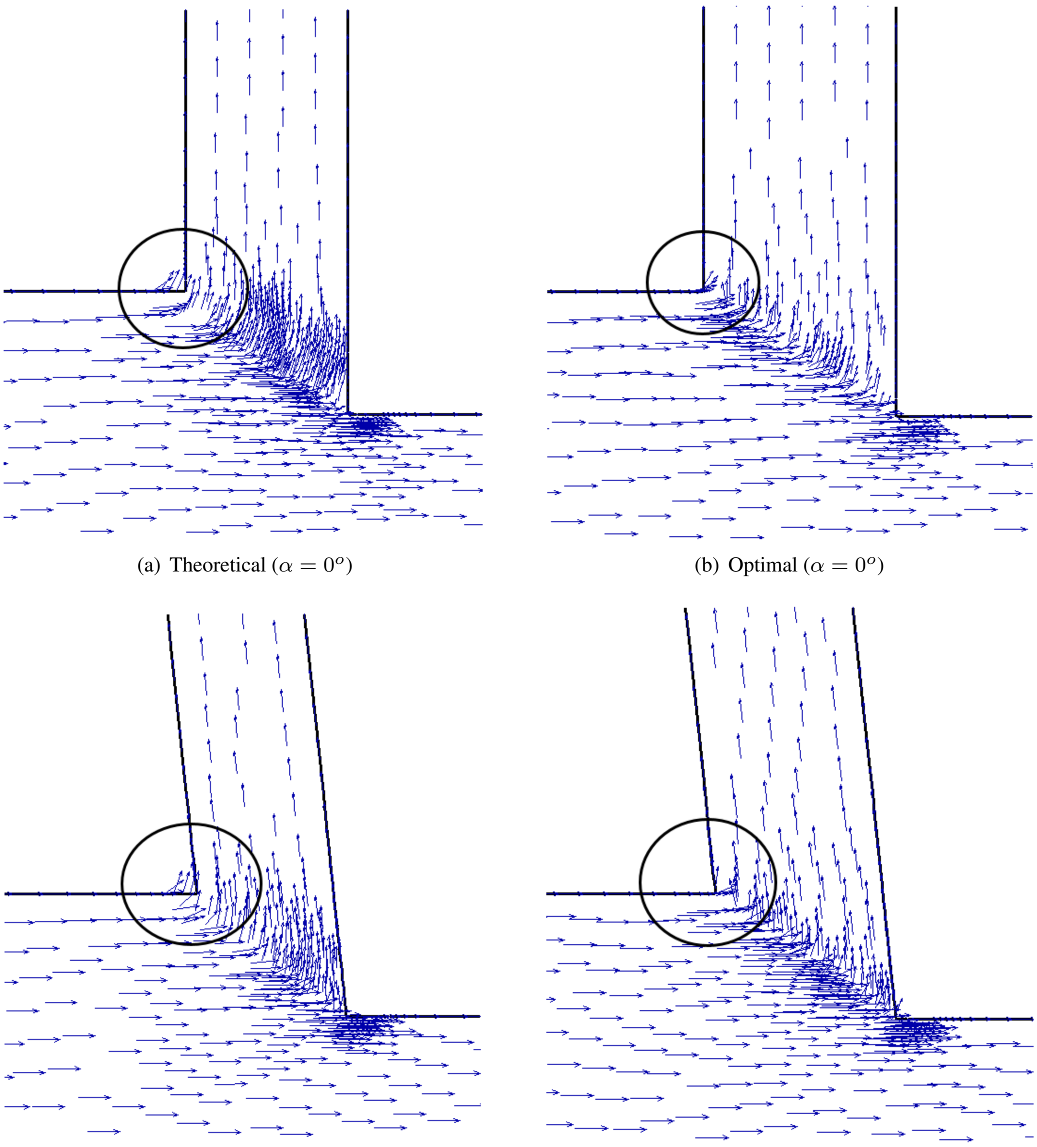

(a) Theoretical ($\alpha = 0^o$) (b) Optimal ($\alpha = 0^o$)

(c) Theoretical ($\alpha = -6^o$) (d) Optimal ($\alpha = -6^o$)

Figure 6. Comparison of theoretical and optimal shear angle configuration velocity fields for geometric l_c.

In Figures 6(a) and 6(c), it was observed that the velocity field obtained for Merchant model do not correspond the the permanent regime configuration. Around point B, the velocity field is not tangent to the geometry. In Figures 6(b) and 6(d), when using the optimal shear angles for rake angles of 0^o and -6^o respectively, the velocity fields exhibit a consistent permanent regime and align with the Merchant proposed configuration. This leads to increased flow stability.

Finally, the comparison for theoretical and optimal shear angle results with the experimental cutting forces were made.

Table 5. Comparison for theoretical and optimal shear angle results with the experimental cutting forces.

α	F_c^{exp} (N)	l_c	ϕ		F_c (N)	Error (%)
0	92.55	Merchant	theoretical	37.081	95.676	-3.38%
			optimal	34.258	95.574	-3.27%
		geometric	theoretical	37.081	95.187	-2.85%
			optimal	32.869	99.781	-7.81%
-6	68.18	Merchant	theoretical	39.37	71.164	-4.37%
			optimal	34.804	72.198	-5.89%
		geometric	theoretical	39.37	72.345	-6.10%
			optimal	34.645	70.604	-3.55%

There were no significant change in the cutting forces results, except for the case $\alpha = 0^o$ and geometric l_c where the error increased from -2.85% to -7.81%, approximately 5%. In the others, the error difference were below to 3% and the minimum was 0.11%.

5. CONCLUSIONS

The use of numerical models combined with experimental methods is important for comprehending the mechanics of metal cutting. Beyond prediction of global quantities as cutting forces, numerical methods allows the study of local phenomena, not captured by experimental device. In this paper, it was presented an analysis of Merchant and Molinari permanent regime configurations to be applied to limit analysis methodology. Both configurations must fit the velocity field determined from the limit analysis problem.

The Merchant model is one of the most used models in the literature to model the orthogonal cutting problems, but when compared to the experimental results it presented discrepancies mainly in the shear angle determination. Based in this problem, Molinari and Moufki model revised the Merchant model proposing to add to the principle of the cutting energy minimization, a stability criterion of the chip morphology. This criterion consists in create a perturbation region in the chip free surface as function of the shape angle and perturbation amplitude, because of this new geometry the authors propose a new shear angle. Normally, the experimental shear angle is smaller than the value found by the Merchant model.

The cutting forces were compared for the two orthogonal cutting configuration, Merchant and Molinari. For the Merchant model, the maximum errors were -3.38% and -6.10%, respectively for the rake angle 0^o and -6^o and for the Molinari model, have the same error variation and was noticed that the shape angle is not much relevance to modify the cutting forces. In both cases, the rake angle variation changes the error, for the Merchant model the case -6^o had the highest errors, in the case of the Molinari the opposite occurred in most cases, when rake angle was -6^o maximum error was 8.80%.

Analyzing the velocity fields on the free surface, the Merchant Model presented velocity filed not tangent to the permanent regime geometry, despite the rake angle values. The same behavior was verified to the Molinari model. When the rake angle is 0^o, the best configuration for the velocity fields was obtained for the shape angle 15^o and for $\alpha = -6^o$ were θ 15^o and 45^o, because the velocity fields was more stable and the flow fit to the permanent configuration.

Besides, this work identifies the deviation between the shear angle predicted by Merchant theory and the optimum one obtained from limit analysis solution. The new angle agrees with the Merchant proposes as shown in the plastic dissipation and the velocity fields results. The comparison for theoretical and optimal shear angle results with the experimental cutting forces, there were no significant change in the results, except for the case $\alpha = 0^o$ and geometric l_c where the error increased from -2.85% to -7.81%, approximately 5%. In the others, the error difference were below to 3% and the minimum was 0.11%.

6. ACKNOWLEDGEMENTS

The authors would like to acknowledge the support of this research by their own institutions, by CAPES (Coordenação de Aperfeiçoamento de Pessoal de Nível Superior) and CNPq (Conselho Nacional de Desenvolvimento Científico e Tecnológico). This work was supported by CAPES (grant number PNPD 31001017030D4) and CNPq (grant number 141627/2009.3).

7. REFERENCES

Almeida, L.P., 2020. "Estudo da usinabilidade de aços inoxidáveis aisi 316, aisi 410 e uns s31803". *Instituto Politecnico de Braganca and CEFET/RJ. Dissertação de mestrado*.

Araujo, A.C., Mougo, A.L. and Campos, F.O., 2020. *Usinagem para engenharia: um curso de mecânica do corte*. E-papers.

Dimas, N.A., 2018. "Modelagem numérico experimental do corte ortogonal". *Universidade Federal do Rio de Janeiro. Projeto Final*.

Ebecken, B.C.F., 2009. "Modelo de análise limite para corte ortogonal". *Universidade Federal do Rio de Janeiro. Projeto Final*.

Ferraresi, D., 1970. *Fundamentos da usinagem dos metais*. E. Blücher.

Figueiredo, F.C. and Borges, L.A., 2017. "Limit analysis formulation for frictional problems". *Archive of Applied Mechanics*, Vol. 87, pp. 1965–1977.

Figueiredo, F.C. and Borges, L.A., 2020. "Limit analysis and frictional contact: formulation and numerical solution". *Meccanica*, Vol. 55, No. 6, pp. 1347–1363.

Gomes, L.A.M., Figueiredo, F.C., Nogueira, L.M. and Mougo, A.L., 2022. "Evaluation of friction at the chip-tool interface in orthogonal cutting by mechanistic models applied to limit analysis". In *Proceedings of the 8th International Symposium on Solid Mechanics*. Campinas, São Paulo.

Groover, M.P., 2012. *Fundamentals of modern manufacturing: materials processes, and systems*. John Wiley & Sons.

Grzesik, W., 2016. *Advanced machining processes of metallic materials: theory, modelling and applications*. Elsevier.

Kato, S., Yamaguchi, K. and Yamada, M., 1972. "Stress distribution at the interface between tool and chip in machining". *Journal of Manufacturing Science and Engineering*, Vol. 94, pp. 683–689.

Melkote, S., Liang, S.Y., Ozel, T., Jawahir, I., Stephenson, D.A. and Wang, B., 2022. "A review of advances in modeling of conventional machining processes: from merchant to the present". *Journal of Manufacturing Science and Engineering*, pp. 1–49.

Merchant, M.E., 1945a. "Mechanics of the metal cutting process. i. orthogonal cutting and a type 2 chip". *Journal of applied physics*, Vol. 16, No. 5, pp. 267–275.

Merchant, M.E., 1945b. "Mechanics of the metal cutting process. ii. plasticity conditions in orthogonal cutting". *Journal of applied physics*, Vol. 16, No. 6, pp. 318–324.

Molinari, A. and Moufki, A., 2008. "The merchant's model of orthogonal cutting revisited: A new insight into the modeling of chip formation". *International Journal of Mechanical Sciences*, Vol. 50, No. 2, pp. 124–131.

Özel, T. and Zeren, E., 2005. "Finite element method simulation of machining of aisi 1045 steel with a round edge cutting tool". pp. 533–542.

Waldorf, D.J., 2006. "A simplified model for ploughing forces in turning". *Journal of manufacturing processes*, Vol. 8, No. 2, pp. 76–82.

8. RESPONSIBILITY NOTICE

The authors are solely responsible for the printed material included in this paper.